Nonlithographic Hierarchical Patterning of Semiconducting Nanoparticles via Polymer/Polymer Phase Separation

C.-W. Wang and Matthew G. Moffitt*

Department of Chemistry, University of Victoria, P.O. Box 3065, Victoria, British Columbia V8W 3V6 Canada

Received March 22, 2005. Revised Manuscript Received May 17, 2005

We demonstrate a new and versatile nonlithographic strategy for the lateral patterning of semiconducting quantum dots (QDs) in thin polymer films via phase separation between two immiscible polymer components, one of which is attached as a stabilizing layer to the QD surface. Simple spin-casting of blend solutions containing block copolymer-stabilized cadmium sulfide (CdS) QDs with an external polystyrene (PS) brush layer (PS−CdS) and poly(methyl methacrylate) (PMMA) homopolymer results in solvent evaporation-induced organization of QDs on two disparate length scales: polymer/polymer spinodal decomposition gives rise to tunable microscopic lateral patterning of PS−CdS features (with mesoscopic feature heights), while simultaneous steric interactions between the polymer brush layers on neighboring nanoparticles give rise to a nanoscale liquidlike distribution of QDs within the PS−CdS domains. The correlation length and morphology of the lateral patterns are easily controlled via the spin-casting rotation speed and blend composition, respectively. Subsequent selective removal of the PMMA component allows the production of various photoluminescent PS−CdS features with structural hierarchy on glass substrates, including cellular and wirelike networks and arrays of spatially correlated islands.

Introduction

Colloidal semiconducting nanoparticles, or quantum dots (QDs), have been recognized as promising building blocks for a new generation of photonic and electronic devices due to their unique and size-dependent properties arising from quantum confinement and surface effects. Essential to the production of devices and materials with specific function will be the organization of QDs on solid substrates into ordered patterns with well-defined length scales. Nonlithographic techniques harnessing spontaneous processes such as dewetting and phase separation offer immense promise for the fast and efficient self-assembly of QDs into regular patterns over large areas. The drying-mediated self-assembly of colloidal nanoparticles deposited from volatile solvents onto various substrates has been found to yield a wide range of surface patterns, including cellular and bicontinuous networks, and arrays of nanoparticle aggregates with strong spatial correlation.[1−8]

Many future materials and devices based on QDs will require their incorporation and organization in polymer environments. Microphase-separated block copolymers have been used to template the organization of QDs, demonstrating excellent control over the spatial distribution of QDs on the length scale of tens of nanometers.[9−13] However, an essential feature of patterning using block copolymers is the inherent connectivity of the phase-separating blocks, which restricts feature sizes to the dimensions of the polymer chains. With the growing need for photonic materials and devices, self-assembly strategies resulting in hierarchical polymer/QD structures with features on micron or just under micron length scales, on the order of optical wavelengths, will be required.

Phase separation of immiscible homopolymer mixtures by casting from a common solvent is a well-established method of forming micrometer surface patterns of two or more polymers on a solid substrate.[14−18] As the solvent evaporates, composition waves develop by spinodal decomposition,

* To whom correspondence should be addressed. E-mail: mmoffitt@uvic.ca.

(1) Ge, G.; Brus, L. *J. Phys. Chem. B* **2000**, *104*, 9573−9575.
(2) Maillard, M.; Motte, L.; Ngo, A. T.; Pileni, M. P. *J. Phys. Chem. B* **2000**, *104*, 11871−11877.
(3) Rabani, E.; Reichman, D. R.; Geissler, P. L.; Brus, L. E. *Nature* **2003**, *426*, 271−274.
(4) Taylor, M. D. R.; Moriarty, P.; Brust, M. *Chem. Phys. Lett.* **2001**, *348*, 27−33.
(5) Mougin, K.; Haidara, H. *Langmuir* **2002**, *18*, 9566.
(6) Martin, C. P.; Blunt, M. O.; Moriarty, P. *Nano Lett.* **2004**, *4*, 2389−2392.
(7) Böker, A.; Lin, Y.; Chiapperini, K.; Horowitz, R.; Thompson, M.; Carreon, V.; Xu, T.; Abetz, C.; Skaff, H.; Dinsmore, A. D.; Emrick, T.; Russell, T. P. *Nature Mater.* **2004**, *3*, 302−306.
(8) Saunders: A. E.; Shah, P. S.; Sigman, M. B.; Hanrath, T.; Hwang, H. S.; Lim, K. T.; Johnston, K. P.; Korgel, B. A. *Nano Lett.* **2003**, *4*, 1943−1948.
(9) Lopes, W. A.; Jaeger, H. M. *Nature* **2001**, *414*, 735−738.
(10) Bockstaller, M. R.; Lapetnikov, Y.; Margel, S.; Thomas, E. L. *J. Am. Chem. Soc.* **2003**, *125*, 5276−5277.
(11) Sohn, B.-H.; Choi, J.-M.; Yoo, S. I.; Yun, S.-H.; Zin, W.-C.; Jung, J. C.; Kanehara, M.; Hirata, T.; Teranishi, T. *J. Am. Chem. Soc.* **2003**, *125*, 6368−6369.
(12) Misner, M. J.; Skaff, H.; Emrick, T.; Russell, T. P. *Adv. Mater.* **2003**, *15*, 221−224.
(13) Yeh, S.-W.; Wei, K.-H.; Sun, Y.-S.; Jeng, U.-S.; Liang, K. S. *Macromolecules* **2003**, *36*, 7903−7907.
(14) Tanaka, K.; Takahara, A.; Kajiyama, T. *Macromolecules* **1996**, *29*, 3232−3239.
(15) Walhein, S.; Böltau, M.; Mlynek, J.; Krausch, G.; Steiner, U. *Macromolecules* **1997**, *30*, 4995−5003.
(16) Ton-That, C.; Shard, A. G.; Daley, R.; Bradley, R. H. *Macromolecules* **2000**, *33*, 8453−8459.
(17) Harris, M.; Appel, G.; Ade, H. *Macromolecules* **2003**, *36*, 3307−3314.
(18) Walheim, S.; Ramstein, M.; Steiner, U. *Langmuir* **1999**, *15*, 4828−4836.

10.1021/cm0506252 CCC: $30.25 © 2005 American Chemical Society
Published on Web 06/22/2005

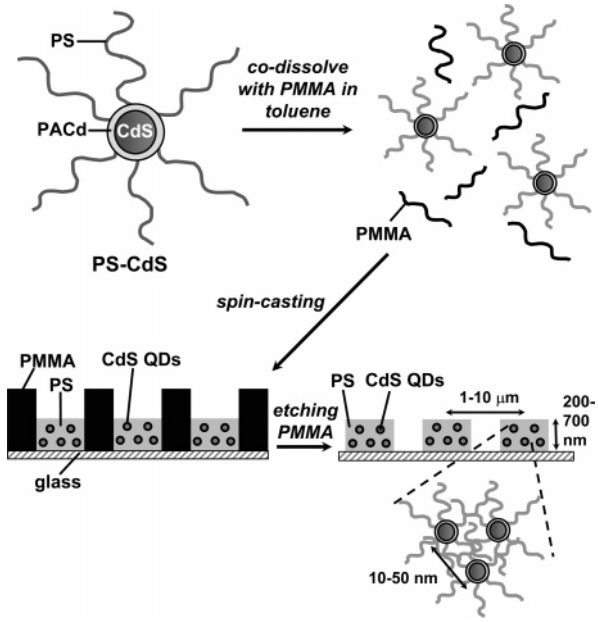

Figure 1. Schematic showing block copolymer-stabilized CdS QD (PS−CdS) and method of patterning by spin-casting PS−CdS/PMMA blends from toluene solutions followed by selective etching of the PMMA domains. The final PS−CdS features show organization on two disparate length scales, as described in the text.

giving rise to various patterns of phase separated polymer domains, with characteristic correlation lengths that depend on the extent of coarsening.[19−21] Lateral patterns formed in this way tend to be isotropic, although nonisotropic structures can be replicated by a combination of polymer/polymer phase separation and selective wetting on a prepatterned substrate.[22,23]

To our knowledge, only one previous study has used polymer/polymer phase separation to direct the assembly of inorganic nanoparticles on a solid substrate.[24] In that work, Amis and co-workers employed a two-step process in which a poly(DL-lactide)/poly(ϵ-caprolactone) blend was first spin cast onto silicon, after which dendrimer-coated cadmium sulfide (CdS) QDs were exposed to the phase-separated film, resulting in selective adhesion of QDs to the surface of the more hydrophilic poly(DL-lactide) domains.[24] Here, we present a new, one-step strategy for the patterning of semiconducting nanoparticles in polymer films, in which QD self-assembly occurs as a result of concurrent phase separation between a polymer joined to the QD surface and an immiscible homopolymer component (Figure 1), resulting in hierarchical structures with QD organization on two length scales.

CdS QDs stabilized by a polystyrene-*b*-poly(cadmium acrylate) (PS-*b*-PACd) block copolymer layer have been synthesized and extensively characterized in our group.[25,26] These stable building blocks are protected by an outer PS brush layer, which governs the interactions of QDs with the surrounding medium, making them soluble in good solvents for PS and completely miscible in PS homopolymer; strong ionic interactions in the PACd layer serve as cross links, locking the block copolymer chains into the brush at the QD surface, even with the removal of solvent.[25,26] In this work, we take advantage of the "PS-like" behavior of these stabilized nanoparticles to induce QD self-assembly via phase separation from an immiscible poly(methyl methacrylate) (PMMA) homopolymer, using simple spin casting of blend components onto glass substrates. A unique feature of this strategy is the use of a single, fast spin-casting step to effect controllable organization of QDs on two disparate length scales in a polymer film: (1) micrometer-scale ordering governed by polymer/polymer phase separation and (2) nanoscale ordering governed by steric interactions between polymer brush-coated QDs.

Experimental Section

Block Copolymer-Stabilized QD Building Blocks. The synthesis and characterization of the block copolymer-stabilized QD sample employed in this work has been previously described.[25,26] The procedure is based on the self-assembly of a polystyrene-*b*-poly(acrylic acid) (PS-*b*-PAA) block copolymer in organic solvents by the addition of cadmium acetate to form polystyrene-*b*-poly(cadmium acrylate) (PS-b-PACd) reverse micelles; the synthesis of a single CdS quantum dot in the core of each micelle was achieved by treatment with H_2S and subsequent ionic cross linking of the PAA layer with cadmium acetate. The starting material for QD synthesis was the amphiphilic block copolymer PS(330)-*b*-PAA(20) ($M_w/M_n = 1.02$), where the numbers in brackets denote number-average degrees of polymerization. The resulting sample is termed PS−CdS (Figure 1),[27] and consists of CdS QDs with average diameter 5.4 nm (determined from the UV−vis absorption onset), protected by an ionically cross-linked surface layer of PACd blocks and an outer brush layer of hydrophobic PS blocks with an average length of 330 styrene repeat units. From light-scattering measurements and assuming that no QD aggregates formed in solution, it was estimated that each PS−CdS particle is decorated with an average of 430 PS chains, giving a brush density of ~1 PS chain/nm^2 on the surface of the particles.[26] The photoluminescence (PL) spectrum of PS−CdS in toluene solution revealed two emission bands, a sharp band-edge emission at 469 nm and a broad trap-state emission centered at 622 nm.[25]

Preparation of Patterned PS−CdS Films. Blends of PS−CdS and PMMA homopolymer (Aldrich, $M_w = 120\,000$ g/mol) were prepared by dissolving appropriate quantities of each component individually in spectroscopic grade toluene to a polymer concentration of 6 wt %. The stock solutions were stirred for ~4 h and allowed to equilibrate overnight in the dark. Blend solutions (6 wt %) of the desired composition were prepared by filtering measured amounts of each solution through two membrane filters (0.45-μm nominal pore size) connected in series into a glass sample vial. As described in the text, three compositions of the polymer blend solutions were made in this manner: PS−CdS/ PMMA (w/w) = 50/50, 30/70, and 10/90.

(19) Ribbe, A. E.; Hashimoto, T. *Macromolecules* **1997**, *30*, 3999−4009.
(20) Takeno, H.; Iwata, M.; Takenaka, M.; Hashimoto, T. *Macromolecules* **2000**. *33*, 9657−9665.
(21) Wang, W.; Shiwaku, T.; Hashimoto, T. *Macromolecules* **2003**, *36*, 8088−8096.
(22) Böltau, M.; Walheim, S.; Mlynek, J.; Krausch, G.; Steiner, U. *Nature* **1998**, *391*, 877−879.
(23) Sprenger, M.; Walheim, S.; Schäfle, C.; Steiner, U. *Adv. Mater.* **2003**, *15*, 703−706.
(24) Gröhn, F.; Gu, X.; Grüll, H.; Meredith, J. C.; Nisato, G.; Bauer, B. J.; Karim, A.; Amis, E. J. *Macromolecules* **2002**, *35*, 4852−4854.
(25) Wang, C.-W.; Moffitt, M. *Langmuir* **2004**, *20*, 11784−11796.
(26) Wang, C.-W.; Moffitt, M. *Langmuir* **2005**, *21*, 2465−2473.
(27) In refs 25 and 26, PS−CdS is referred to as MIC−CdS4.

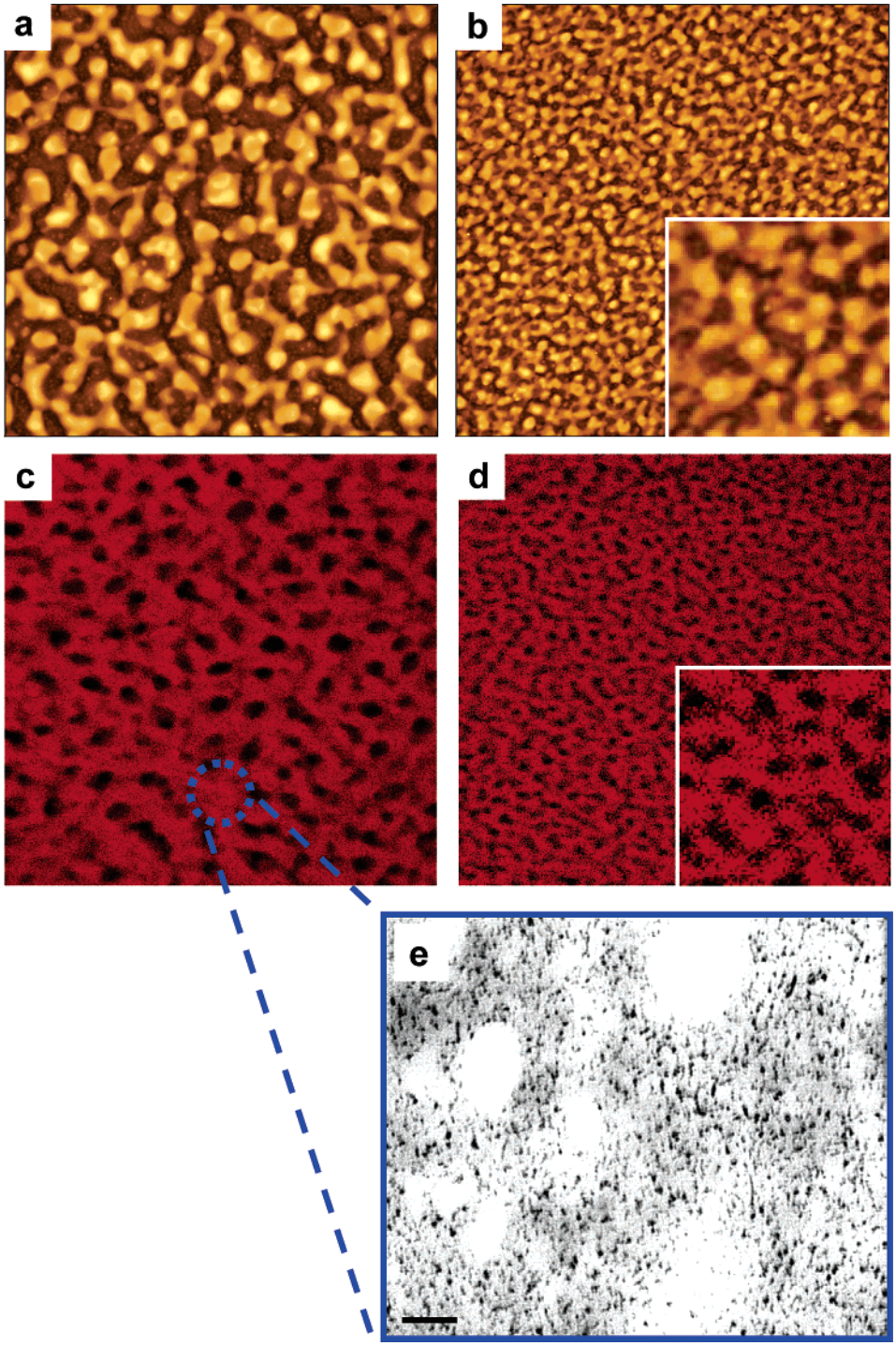

Figure 2. AFM (a,b) and LSCFM (c,d) images of spin-cast 50/50 (w/w) PS−CdS/PMMA blend films, prepared using rotation speeds of 3000 rpm (a,c) and 9000 rpm (b,d). All AFM and LSCFM images have edge lengths of 50 μm; the insets have edge lengths of 10 μm and show enlarged regions of the 9000 rpm film from images in b and d. TEM image (e) of the microtomed 3000 rpm blend, showing the nanoscale organization of QDs within the photoluminescent PS−CdS domains; the scale bar in the TEM image represents 100 nm.

The blend films were made by spin casting one drop of the blend solution onto clean 18 × 18 mm glass coverslips at different rotation speeds (3000, 6000, and 9000 rpm) for one minute. Before spin casting, the glass substrates were cleaned by 10 min sonication in chloroform, followed by 10 min sonication in methanol, then overnight drying under vaccum. To test reproducibility, several films were prepared for each composition and speed of rotation. Before imaging, all films were placed in a vacuum oven and dried overnight under active vacuum at room temperature to remove any residual solvent.

Selective removal of the PMMA phase (etching) was carried out by placing the films in a Petri dish containing acetone and a stir bar and stirring for 4−5 min. The films were then removed and further rinsed with acetone, before air drying for 3−4 h followed by drying under active vacuum at room temperature (RT) overnight. Spin-cast PS−CdS/ PMMA films were mainly transparent in appearance before etching, but became markedly turbid after etching.

Atomic Force Microscopy (AFM). All AFM images were obtained using a Veeco Instrument equipped with a Veeco tip

(Nanoprobe-MLCT-EXMT-A) and operating in contact mode. To minimize the effect of vibrations, the AFM probe was covered with a vibration-resistant case on a vibration isolation platform maintained at 80 psi. Each sample was imaged several times at different locations on the substrate to determine the regularity of patterning.

Laser Scanning Confocal Fluorescence Microscopy (LSCFM). Laser scanning confocal fluorescence microscopy measurements were carried out on on a Zeiss LSM 410 equipped with an Ar/Kr laser. All films were excited at ~488 nm, using a band-pass 485 ± 20 nm line selection filter and a FT 510 dichroic beam splitter. A long-pass 515 emission filter was used such that only light above 515 nm reached the PMT. A pinhole diameter 1.31 Airy Units was used for all measurements, resulting in an optical section thickness of 0.75 μm fwhm.

Transmission Electron Microscopy (TEM). TEM was performed on a Hitachi H-700 electron microscope, operating at an accelerating voltage of 70 kV. Selected spin-cast CdS/ PMMA films, before and after etching, were embedded in an Epon resin, and then ~60 nm thick sections were produced with a diamond knife on Reichert UltraCut E ultra-microtone. The thin sections were placed on carbon/Formvar-coated 300 mesh copper grids for imaging.

Results and Discussion

To produce patterned polymer/QD films, various blend solutions of PS−CdS and PMMA homopolymer in toluene (total concentration = 6 wt %) were spin cast onto glass substrates. PS−CdS and PMMA are both completely soluble in toluene and form a single transparent phase in solution; however, as the solvent evaporates during spin-casting, the immiscibility of the outer PS layer and the PMMA homopolymer leads to phase separation, resulting in self-assembly of polymer-coated QDs. For 50/50 (w/w) PS−CdS/ PMMA blends, spin-casting was carried out at rotation speeds of 3000, 6000, and 9000 rpm, giving films ranging from 250 to 650 nm in thickness, with thicker films resulting from slower rotation speeds. The surface morphologies of the resulting films were determined by AFM in contact mode, revealing spontaneous patterning arising from spin casting. The AFM image of the 3000 rpm film (Figure 2a) shows a clear bicontinuous structure of raised (light) and lower (dark) domains, while the 9000 rpm film shows a similar lateral pattern (Figure 2b, inset) but on a smaller length scale; the 6000 rpm film (not shown) revealed the same bicontinuous domain structure, with feature sizes between those of the 3000 and 9000 rpm films. Smaller lateral feature sizes for faster rotation speeds can be explained by a faster rate of solvent evaporation, which results in the blend films being kinetically trapped at earlier stages of domain coarsening. The combination of bicontinuous domain structure and structural self-similarity for different stages of phase coarsening strongly suggests that lateral patterning occurs by a mechanism of spinodal decomposition between immiscible PS−CdS and PMMA components.[21] Along with the observed lateral features, AFM indicates that the blend films exhibit a topology coinciding with the domain structure, in which one phase protrudes above the other at the film surface; a similar phenomenon has been observed previously in more conventional blends of PS and PMMA homopolymers spin cast from toluene[14,15] and was attributed to the preferential solubility of PS in toluene relative to PMMA.[15] In the present case, the PS−CdS phase will be more highly swollen with toluene than the PMMA phase as the lateral domain structure develops, eventually collapsing below the level of the PMMA domains when the last of the solvent evaporates (Figure 1). For AFM surface morphologies in parts a and b of Figure 2, therefore, we infer that the raised features are comprised of PMMA, and the lower features consist of self-assembled PS−CdS QDs; further evidence for this domain assignment is discussed below.

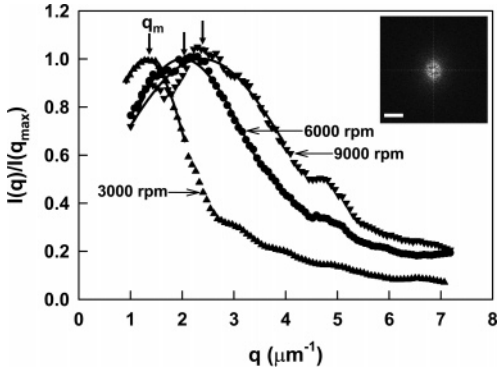

Figure 3. Plots of normalized intensity $I(q)/I(q_m)$ vs scattering vector q, from radially averaged 2D-FFT of LSCFM images of 50/50 (w/w) PS−CdS/PMMA blends, prepared using rotation speeds of 3000, 6000, and 9000 rpm. The solid lines show a simple Gaussian fit of the resulting peaks and arrows indicate the peak maxima q_m; the peak positions are found to shift to higher q values with increasing rotation speed, demonstrating tunability of the correlation lengths of the patterns. The inset shows a sample 2D-FFT of the LSCFM image in Figure 2c (3000 rpm film); the scale bar represents 5 μm^{-1}.

More direct evidence of lateral QD patterning comes from LSCFM of the blend films, in which contrast is provided by PL from the CdS QDs; all LSCFM images were obtained by excitation of the CdS QDs at 488 nm and collection of light from the red-shifted trap-state emission (>515 nm). LSCFM images of the 3000- and 9000-rpm films (parts c and d of Figure 2, respectively) show regular patterns of photoluminescent PS−CdS domains (red regions) with feature sizes corresponding to the AFM images, along with analogous self-similarity at different rotation speeds (Figure 2d, inset); this suggests that the self-assembly and patterning of PS−CdS is a result of the same polymer/polymer spinodal decomposition process responsible for the surface morphologies observed by AFM. Despite similarities in the structural information obtained by AFM and LSCFM, we note that AFM probes the topology of the films, whereas LSCFM images the films below the surface. An apparent consequence of this difference in the two imaging techniques is that AFM shows a laterally continuous PMMA phase (light regions, parts a and b of Figure 2), whereas the PMMA domain structure is noncontinuous in the LSCFM images (dark regions, parts c and d of Figure 2); this suggests that the protruding PMMA features at the film surface occupy a larger fraction of the in-place area than the nonprotruding PMMA domains underneath.

Because of the effects of fast solvent evaporation, PS−CdS patterns obtained by spin-casting are not in thermodynamic equilibrium, although they are stable, kinetically "frozen" structures, well below the glass transition temper-

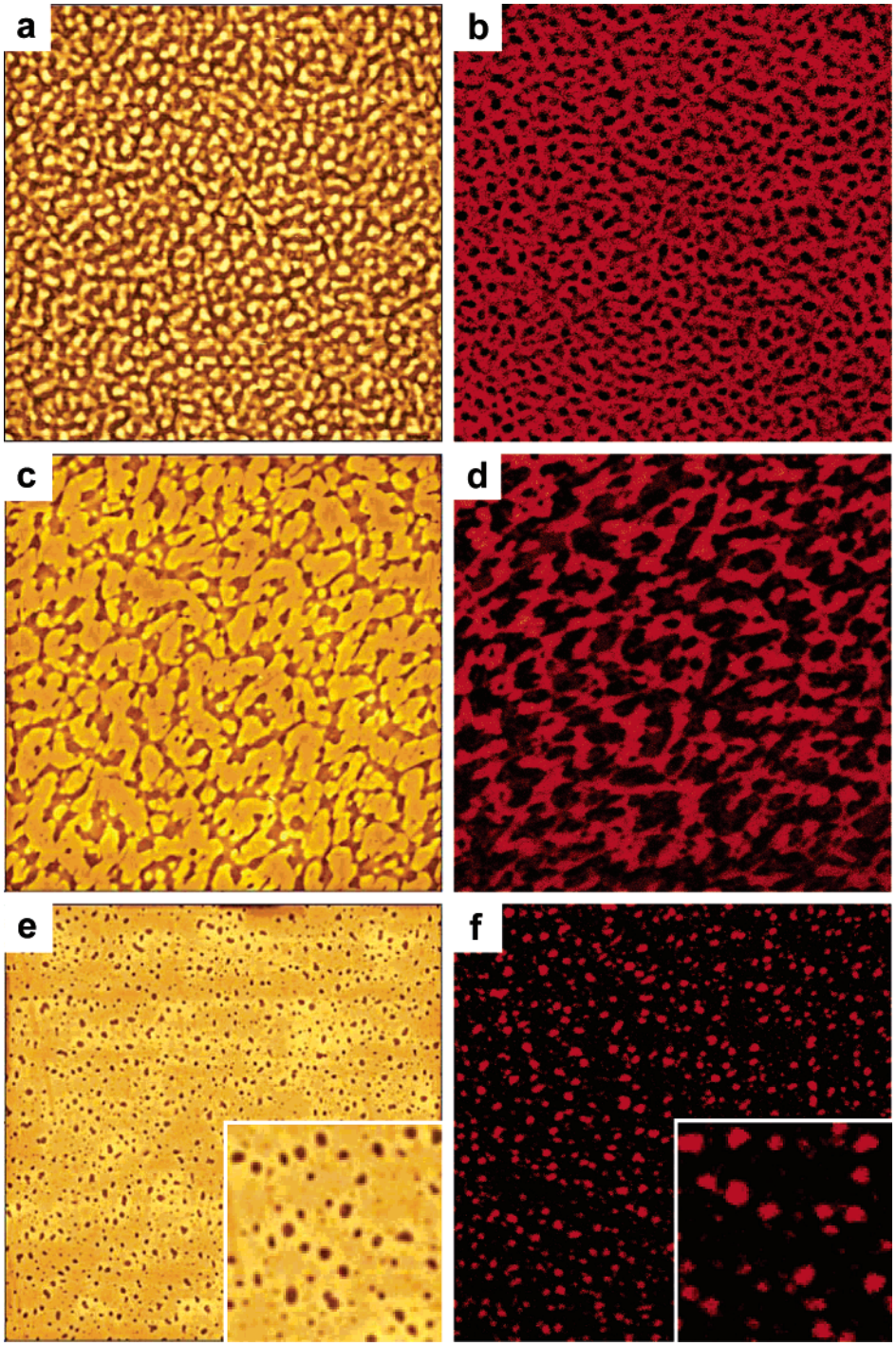

Figure 4. AFM (a,c,e) and LSCFM (b,d,f) images of spin-cast films for various blend compositions: PS−CdS/PMMA (w/w) = 50/50 (a,b); PS−CdS/PMMA (w/w) = 30/70 (c,d); and PS−CdS/PMMA (w/w) = 10/90 (e,f). The edge length of all images is 100 μm. For all blend compositions, the rotation speed for spin casting was 3000 rpm. Insets (edge length = 20 μm) show enlarged regions of the 10/90 sample from images in e and f.

atures of both polymer components in the absence of solvent. We have seen that the kinetic nature of these patterns allows the length scale of QD organization to be easily tuned via the spin-casting speed of rotation. To better characterize the order and characteristic correlation lengths of PS−CdS patterns obtained at different rotation speeds, two-dimensional fast Fourier transforms (2D-FFT) of binarized LSCFM images of the various films were obtained. Radial averages of 2D-FFT images yield plots of intensity $I(q)$ vs scattering vector q, which are equivalent to 2D structure factors. 2D-FFT of LSCFM images of 50/50 PS−CdS/PMMA films obtained at 3000, 6000, and 9000 rpm each show a ring (e.g., Figure 3, inset), or a peak in the resulting radial average, indicating PS−CdS organization with well-defined correlation lengths.[6] From the normalized radial averages, $I(q)/I(q_m)$ vs q (Figure 3), it is clear that the peak position shifts to higher q values with increasing speed of rotation. Simple Gaussian fits of each of these plots were used to determine the peak positions q_m, from which a characteristic correlation length, $\Lambda_m = 2\pi/q_m$, was obtained for each lateral pattern, giving $\Lambda_m = 4.8$, 3.1, and 2.6 μm for the 3000, 6000, and 9000 rpm films, respectively. These values agree well with estimated average feature spacings from LSCFM images of the patterned films (parts c and d of Figure 2).

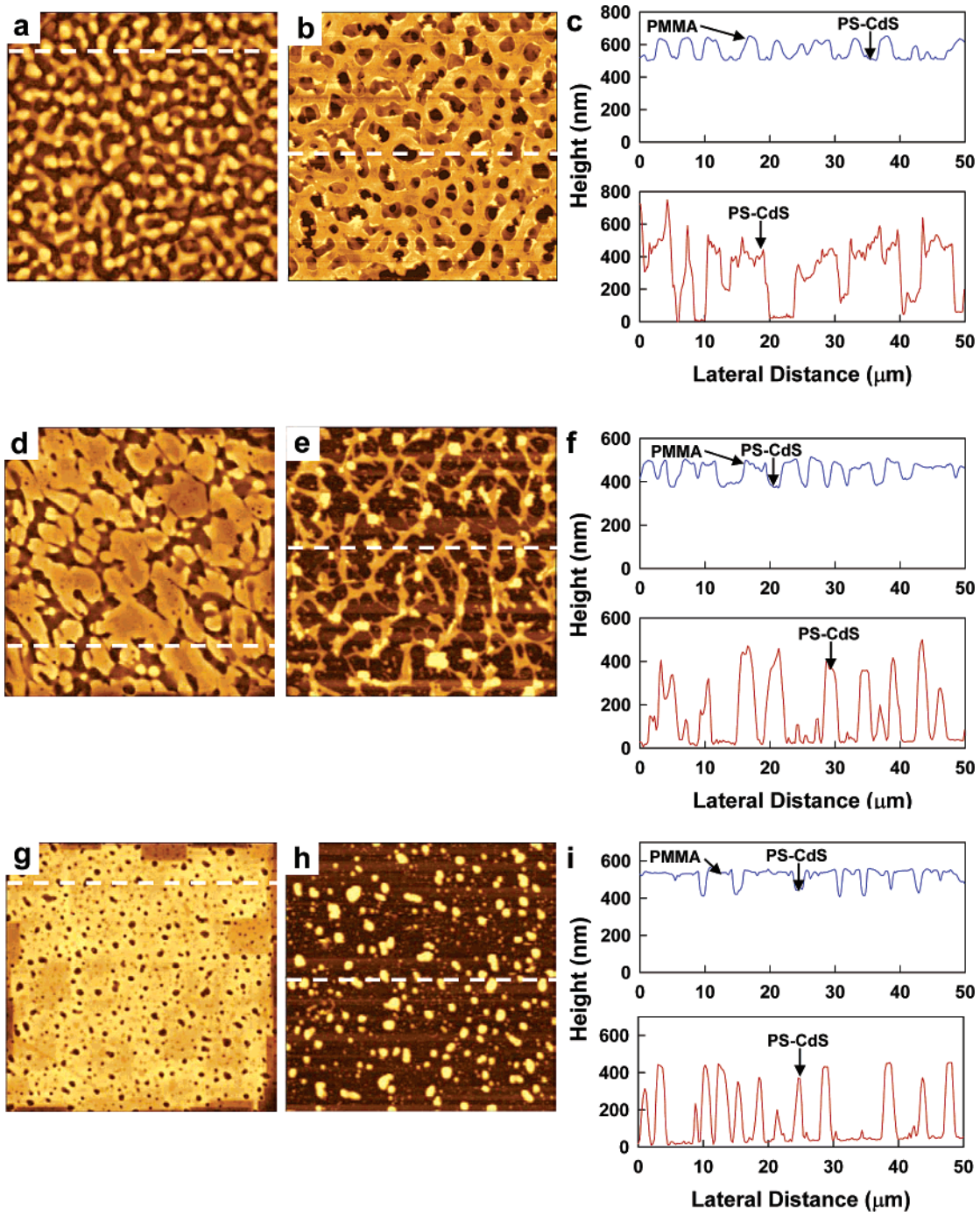

Figure 5. AFM images and topographic cross sections of 3000-rpm spin-cast films for various blend compositions, before (a,d,g) and after (b,e,h) selective removal of the PMMA phase by etching with acetone: PS−CdS/PMMA (w/w) = 50/50 (a−c); PS−CdS/PMMA (w/w) = 30/70 (d−f); and PS−CdS/PMMA (w/w) = 10/90 (g−i). The edge length of all images is 50 μm. For each composition, topographic cross sections (c,f,i) are shown before (upper, blue line) and after (lower, red line) removal of PMMA. Cross sections before etching are shifted up by the value of the average feature height following etching, so that zero height represents the substrate in all cases.

To determine the specific organization of QDs within the PS−CdS domains, microtomed sections of the spin-cast films were obtained and mounted on grids for transmission electron microscopy (TEM). From sections of the 50/50 PS−CdS/PMMA film (3000 rpm), TEM (Figure 2e) clearly shows the nanoscale spatial distribution of QDs within the PS matrix of the PS−CdS phase, highlighting the structural hierarchy in these films. No long-range order of QDs is discernible, though the inorganic nanoparticles are well dispersed and quite evenly spaced, suggesting that QDs are spatially distributed in a liquidlike fashion. While the micrometer-scale ordering observed by AFM and LSCFM is a result of polymer/polymer spinodal decomposition, the nanoscale liquidlike ordering of QDs can be attributed to interactions between PS brush-stabilized nanoparticles within the solvent-swollen PS−CdS phase as the toluene evaporates. Importantly, both levels of organization arise from a single process of solvent evaporation. The ordering of block copolymer micelles at increasing concentrations has been characterized by McConnell and Gast,[28] who found that micelles formed

(28) McConnell, G. A.; Gast, A. P. *Macromolecules* **1997**, *30*, 435−444.

long-range cubic crystals above a critical ordering concentration, but then melted to a less-ordered liquidlike state at even higher concentrations; this melting transition was explained by overlap between the brush layers of neighboring micelles, which resulted in a loss of the osmotic pressure gradient within the brushes and a consequential loss of the repulsive interparticle force. A similar evolution of nanoparticle organization in the PS−CdS phase is envisioned in the present case, where the PS brush layers surrounding self-assembling QDs eventually form the PS matrix observed in Figure 2e upon evaporation of solvent. From the measured PS−CdS aggregation number in toluene and the bulk PS density, the average spacing between CdS QDs is calculated to be 30 nm; this value seems reasonable based in Figure 2e, but is unfortunately difficult to confirm from the obtained microtomed sections, which are not monolayers and therefore represent a superposition of several layers of nanoparticles in the plane of the image. Along with the spatial distribution of QDs, TEM also shows a second population of smaller (100−200 nm) PMMA domains (white regions in Figure 2e), dispersed throughout the PS−CdS phase, which was not visible by LSCFM. These smaller PMMA droplets may be related to the presence of a small amount of free polystyrene-*b*-poly(acrylic acid) (PS-*b*-PAA) from the PS−CdS sample, which could localize at the droplet interface resulting in interfacial stabilization and a slower rate of coarsening compared to the larger PMMA features.

While variation in the spin-casting speed of rotation allowed pattern feature sizes to be easily tuned, different types of PS−CdS patterns could be obtained by varying the blend composition. In addition, analysis of films of different blend compositions provides additional information for the assignment of domains observed by AFM and LSCFM. Figure 4 shows AFM and LSCFM images of films obtained at 3000 rpm with the following PS−CdS/PMMA (w/w) ratios: 50/50 (parts a and b of Figure 4), 30/70 (parts c and d of Figure 4), and 10/90 (parts e and f of Figure 4), revealing a range of nanoparticle patterns, each extending over large areas. Importantly, Figure 4 shows that the relative area of the raised domains observed by AFM increases with the PMMA content of the blend; as well, the lateral patterns of photoluminescent PS−CdS features in the LSCMF images match the lower regions of the corresponding AFM image. These observations provide further evidence for protruding PMMA surface domains which coincide with the lateral features of a subsurface PS−CdS/PMMA domain morphology. 2D-FFT of LSCFM images for the three compositions each showed a ring, indicating well-defined correlation lengths for all of the micron-scale patterns. With decreasing PS−CdS content, the resulting patterns vary from a cellular or foamlike network (50/50, Figure 4b), to a network of PS−CdS wires (Figure 4d), to an array of PS−CdS islands (Figure 4f). The strong spatial correlation of the islands is indicated by their organization into strings (parts e and f of Figure 4, insets), attributed to a spinodal decomposition pathway for pattern formation, in which a continuous network breaks into discrete domains during coarsening.[20]

Finally, we demonstrated that the PMMA component of these films could be selectively removed by etching with

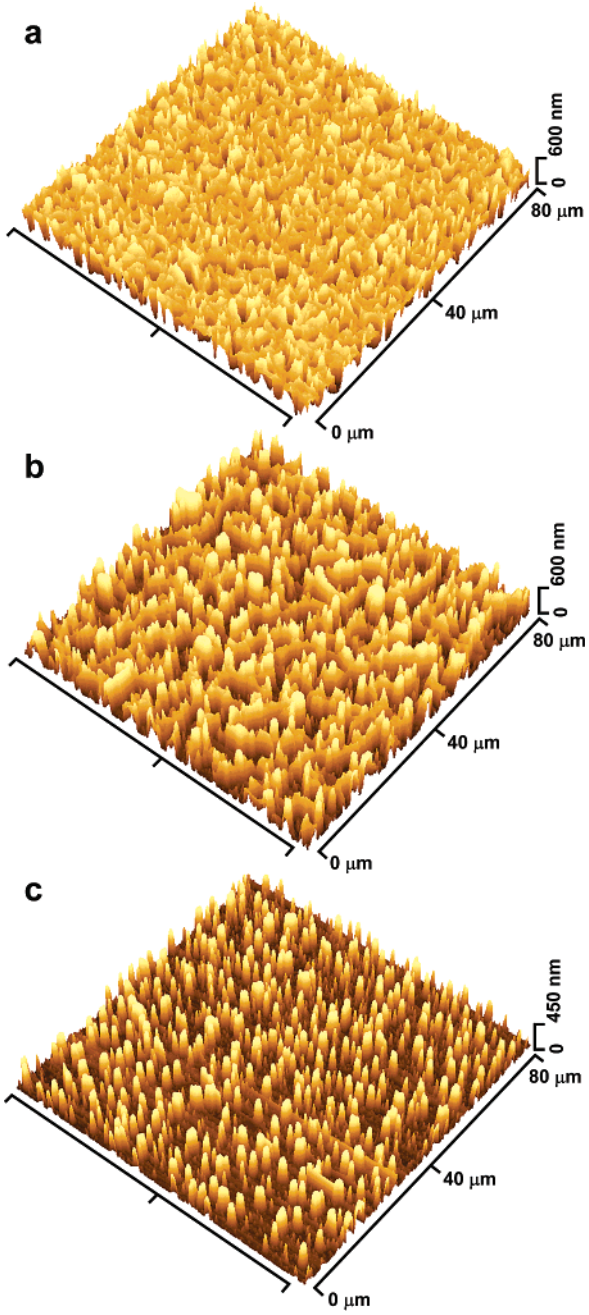

Figure 6. 3D AFM images of patterned PS−CdS films obtained by spin-casting various PS−CdS/PMMA blends at 3000 rpm followed by selective removal of PMMA: PS−CdS/PMMA (w/w) = 50/50 (a); PS−CdS/PMMA (w/w) = 30/70 (b); and PS−CdS/PMMA (w/w) = 10/90 (c).

acetone, a good solvent for PMMA but a poor solvent for PS, leaving behind PS−CdS features with structural hierarchy patterned on glass, as depicted in Figure 1. Figure 5 shows AFM images for 3000 rpm films obtained from different blend compositions, before and after selective dissolution of the PMMA phase. It is evident that the lateral PS−CdS domain morphologies are well preserved after etching, although the film topologies are completely changed by removal of PMMA, with raised regions of the etched films corresponding to the laterally patterned PS−CdS features and low regions corresponding to the glass substrate (Figure 5). An analysis of cross sections of the AFM images before and after removal of PMMA (Figure 5) provides a topographical profile of the PS−CdS/PMMA films, confirming the pres-

ence of protruding PMMA domains at the film surface following spin casting.

Three-dimensional (3D) representations of AFM images for various patterned PS−CdS films after removal of PMMA are shown in Figure 6. Some of the obtained surface structures are particularly interesting, including a continuous network of PS−CdS wires on glass (Figure 6b) with average wire thickness of 1.5 ± 0.5 μm and average height of 370 ± 60 nm, and an array of spatially correlated PS−CdS islands (Figure 6c), with average island diameter of 2.0 ± 0.4 μm and average height of 410 ± 70 nm. Along with the lateral organization visible by AFM, all of the surface features in Figure 6 possess an internal structure of QDs dispersed in a liquidlike fashion, similar to that shown in Figure 2e; from the measured average dimensions of the islands in Figure 6c, and assuming cylindrical geometry, we calculate that each PS−CdS island contains an average of 5.1×10^4 QDs. Importantly, both the lateral dimensions and heights of these features can be tuned via the speed of rotation, choice of solvent, or concentration of the blend solution, offering the potential for making a range of structures with dimensions commensurate with specific applications (e.g., optical wavelengths). For example, by varying the rotation speed from 3000 to 9000 rpm, the average feature height in the etched 50/50 blend films was reduced from 500 ± 90 nm to 200 ± 40 nm. In addition, by varying the length of PS chains on the colloidal PS−CdS building blocks, this strategy offers the possibility of tuning the average spacing of QDs and the number of QDs per unit volume within the various features, independent of the morphology and correlation length of the surface pattern.

The main PL features of PS−CdS quantum dots, characterized previously in dilute toluene solution,[25] are retained in the patterned films, both before and after etching with acetone. Figure 7 shows the PL spectra of spin-cast PS−CdS/PMMA films before and after removal of the PMMA phase, revealing in both cases a sharp band-edge emission at ~470 nm and a broad trap-state emission centered at ~625 nm, very close to the peak positions obtained for PS−CdS in toluene;[25] a slight broadening and blue shift in the band-edge emission is found following etching, which may be due to increased light scattering from the etched films due to a higher refractive index contrast between PS−CdS and air compared to PS−CdS and PMMA. LSCFM of the various films following removal of PMMA also confirmed that the self-assembled QD patterns retain their PL following etching, as shown by the LSCFM image for the etched 10/ 90 PS−CdS/PMMA film (Figure 7, inset).

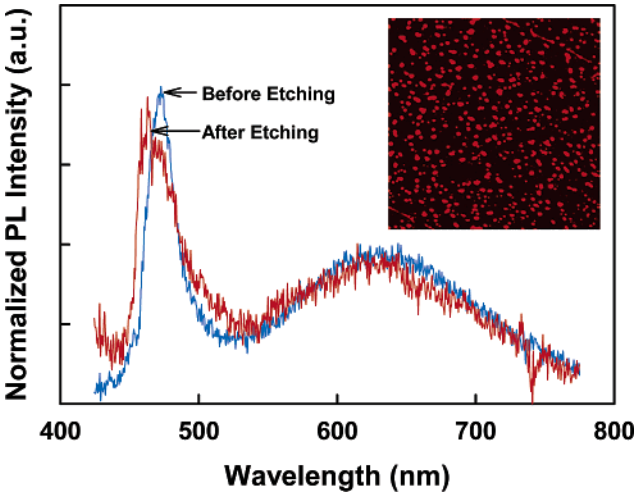

Figure 7. PL spectra (λ_{ex} = 400 nm) of the spin-cast 50/50 PS−CdS/PMMA film obtained at 9000 rpm, before and after removal of PMMA by etching with acetone. The PL peak positions are similar to those obtained previously for PS−CdS in toluene (ref 25). The inset shows the LSCFM image of the PS−CdS/PMMA (w/w) = 10/90 (3000 rpm) film after etching, showing that the PL of the PS−CdS features is retained; the edge length of the inset is 100 μm.

Conclusion

We have demonstrated a novel and versatile strategy for the fast and efficient lateral patterning of semiconducting QDs in thin polymer films via spinodal decomposition between two polymer blend components, one of which is attached as a polymer brush layer to the QD surface. Simple spin casting and solvent evaporation induces simultaneous organization of QDs on two disparate length scales, with polymer/polymer phase separation giving rise to tunable microscopic lateral patterning (with mesoscopic feature heights), and steric interactions between the polymer brush layers of neighboring QDs giving rise to a liquidlike distribution of QDs on the nanoscale. Subsequent selective removal of the PMMA component allows the production of various photoluminescent PS−CdS patterns with structural hierarchy on glass substrates.

Acknowledgment. The authors gratefully acknowledge the National Science and Engineering Research Council, the Canadian Foundation for Innovation, and the British Columbia Knowledge Development Fund for their generous support of the research. We also thank Dr. Robert Burke for assistance with the LSCFM measurements.

CM0506252